Metallurgical and Materials Engineering *Scientific paper*
Association of Metallurgical Engineers of Serbia AMES *UDC: 621.791:669.018.25*

THE INFLUENCE OF CHEMICAL COMPOSITION ON MICROSTRUCTURE, HARDNESS AND ELECTRICAL CONDUCTIVITY OF Ag-Bi-In ALLOYS AT 100 °C

Vladan Ćosović[1], Duško Minić[2], Milena Premović[2], Dragan Manasijević[3], Aleksandar Đorđević[2], Dušan Milisavljević[2], Aleksandar Marković[2]*

[1] University of Belgrade, Institute of Chemistry, Technology and Metallurgy, Belgrade, Serbia
[2] University of Priština, Faculty of Technical Science, Kos. Mitrovica, Serbia
[3] University of Belgrade, Technical Faculty, Bor, Serbia

Received 10.03.2017
Accepted 29.03.2017

Abstract

Considering possible applications and scarceness of literature data, Ag-Bi-In system was investigated in terms of microstructure, mechanical and electrical properties of ternary alloys from an isothermal section at 100 °C. Based on the experimentally obtained results hardness and electrical conductivity of all ternary alloys from the ternary Ag-Bi-In system at 100 °C were predicted. In addition, the selected isothermal section was further thermodynamically assessed and experimentally studied using scanning electron microscopy (SEM) with energy dispersive spectrometry (EDS), X-ray powder diffraction (XRD) analysis and light optical microscopy (LOM). Phase transition temperatures of alloys with overall compositions along vertical sections x(Ag)=0.5 as well as liquidus temperatures were experimentally determined by DTA. The experimentally obtained results were compared with literature data and with the results of thermodynamic calculation of phase equilibria based on CALPHAD method and corrected data for Ag-In binary system. Calculated liquidus projection, invariant equilibria and phase diagram of the Ag-Bi-In ternary system are presented as well.

Keywords: *Ag-Bi-In system; thermodynamic assessment; microstructural analysis; hardness; electrical conductivity.*

Introduction

In the past decade, a lot of research work has been done to find promising free-lead solder materials [1-4]. According to literature tin based alloys may be an adequate replacement for classical lead solders. So far, a quaternary alloy 84Sn-3Ag-3Bi-10In (in

[*] Corresponding author: Vladan Ćosović, *vlada@tmf.bg.ac.rs*

wt.%) seem to be the best alternative among the selection of Pb-free solder systems [5]. In line with that, in recent years there has been quite a few thermodynamic studies on phase diagrams of four ternary systems (Ag-Bi-In [6,7], Ag-Bi-Sn [8,9], Ag-In-Sn [10,11] and Bi-In-Sn [12,13]) that make a quaternary Ag-Bi-In-Sn system.

The ternary Ag-Bi-In system has been previously investigated by *Sabbar et al.* [6], *Vassiliev et al.* [7], *Liu et al.* [14] and *Kameda and Yamaguchi* [15]. In their study *Sabbar et al.* [6] determined enthalpy of formation for alloy samples with compositions along six isoplethic sections x(Bi):x(In)=1:4, x(Bi):x(In)=1:2, x(Bi):x(In)=1:1, x(Bi):x(In)=62:38, x(Ag):x(Bi)=1:3 and x(Ag):x(In)=1:1 in a temperature range 809 to 911 K using a high temperature microcalorimeter. As a result, the enthalpy of formation of liquid can be correctly represented by the Toop relation over the entire ternary molar fraction range.

Activities of indium in liquid Ag–Bi–In alloys were studied both by *Vassiliev et al.* [7] and *Kameda and Yamaguchi* [15]. *Vassiliev et al.* [7] investigated a part of the ternary system x(Ag)=0.5 using differential thermal analysis and potentiometric measurements in a temperature range 630 K to 850 K. They have determined some points of the liquid surface and compared them with the results of potentiometric measurements. *Kameda and Yamaguchi* [15] measured the activities along three isoplethic sections x(Bi):x(Ag)=4:1, x(Bi):x(Ag)=1:1 and x(Bi):x(Ag)=1:4 in a temperature range 896 to 1297 K and based on obtained results proposed iso-activity curves at 1100 and 1200 K.

Phase diagram of a ternary Ag-Bi-In system was investigated by *Liu et al.* [14]. In the same study two isothermal sections at 200 °C and 300 °C°C, vertical section at 50 mass% Ag, liquidus surface and calculated surface tension and viscosity of liquid phase were reported. Isothermal sections at 200 °C and 300 °C were experimentally studied using electron probe microanalysis (EPMA) while the liquid lines and phase transition temperatures of the vertical section at 50 mass% Ag were determined by differential scanning calorimetry (DSC). Based on experimentally obtained results, thermodynamic parameters for ternary liquid phases were assessed.

To our knowledge, so far Ag-Bi-In ternary system has not been investigated in terms of mechanical and electrical properties of ternary alloys from the isothermal section at 100 °C. Such properties are rather important from the application point of view as they provide direct insight into possible applications of these ternary alloys. Besides investigation of mechanical and electrical properties in the current study are also given experimental results of DTA analysis for vertical section x(Ag)=0.5, which were compared with the data reported by *Liu et al.* [14]. Moreover, isothermal section at 100 °C was investigated using SEM-EDS and XRD analysis and a liquidus surface and invariant reactions of the ternary Ag-Bi-In system were calculated and presented as well.

Experimental

All investigated alloy samples were prepared from Ag, Bi, and In with 99.99 at% purity in an induction furnace under high-purity argon atmosphere. The average loss of mass during melting of the samples was about 2 mass%. The samples selected for investigation of isothermal section at 100 °C were placed in evacuated quartz tubes and then sealed. After that, the prepared samples were heated to a temperature that is 50 ºC higher than the melting point of Ag and then cooled to 100 °C at a cooling rate of 5

°C/min. The samples were then annealed at 100 °C for 3 weeks and subsequently quenched into an ice/water mixture in order to preserve the obtained phase equilibriums. It was found that low melting points of the used metals and fast diffusion rates led to equilibrium compositions after applied annealing time (3 weeks). Longer annealing times did not provide any further development of microstructure.

Phase transition temperatures were determined by the DTA method using TA Instruments SDT Q600 thermal analyzer. The samples weighing between 10 and 15 mg were placed in alumina crucibles and analyzed at a heating rate of 5 K (5 °C)/min. The sample masses and heating rates were determined by analysis of a one sample under different testing conditions. The measurements were carried out under flowing nitrogen atmosphere with an empty alumina crucible as reference material.

Microstructural analysis was carried out using JEOL (JSM6460) scanning electron microscope equipped with Oxford instruments energy dispersive spectrometer and using OLYMPUS GX41 inverted light metallographic microscope.

XRD patterns of the studied samples were recorded on Bruker D2 PHASER powder diffractometer fitted out with a dynamic scintillation detector and ceramic Cu tube (KFLCu-2K) in a 2 h range of 5 to 75 deg with a step size of 0.02 deg. The patterns were analyzed using Topas 4.2 software and ICDD databases PDF2 (2013).

The hardness of the samples was determined using Brinell hardness tester Innovatest Nexus 3001. The microhardness of the phases present in the microstructure was determined using Vickers microhardness tester Sinowon Vexus ZHV-1000V by applying load of 0.245 N for 20 s. Electrical conductivities of the studied alloy samples were measured using Foerster SIGMATEST 2.069 eddy current instrument.

Phase equilibria were predicted by thermodynamic calculations based on CALPHAD (CALculation of PHAse Diagrams) method using Pandat 8.1 software.

Literature data

Three constitutive binary systems have been investigated extensively in recent years by many research groups [16-21]. However, in case of Ag-Bi and Bi-In binaries these investigations have not resulted in any changes of phase diagrams. In contrast, investigations performed on binary Ag-In have resulted in some changes of a phase diagram.

Individual intermetallic phases ($\zeta(Ag_3In)$, $\gamma(Ag_2In)$, $\beta(Ag_3In)$ and $AgIn_2$) were initially studied by *Weibke* [22], *Hellner* [23], *Frevel and Ott* [24] and *Campbell* [25]. Even so, the first assessment of an Ag-In phase diagram was carried out by *Baren* [26]. Additional thermodynamic assessment of this system was carried out by *Kornenhen and Kivilahti* [27]. Nevertheless, a close agreement between calculated and experimental results with regard to the phase equilibria associated with ζ phase was not obtained. The most recent assessment of an Ag-In phase diagram was done by *Moser et al.* [28]. Yet, in this study the β (bcc) phase was not considered because of a very small solubility and also a solubility of Ag in In was not taken into account. In addition, an intermetallic compound $\gamma(Ag_2In)$ was considered as a stoichiometric compound.

The most complete phase diagram up to now has been described in COST 531 Lead-free Solders Thermodynamic Database [1]. In data set given in COST 531 database, primary data for Liquid, Ag (Fcc_A1), ζ(Hcp_A3) and $AgIn_2$ phases were taken from *Moser et al.* [28] while model for γ (Ag_2In) in CUIN_GAMMA was

changed in order to improve necessary solubility. Moreover, in order to correctly model the liquidus surface, β(Ag_3In) phase was also added. The inclusion of (β(Ag_3In)) phase has instigated one extra invariant reaction. A phase diagram of the binary Ag-In system calculated using COST 531 data is presented in Fig. 1.

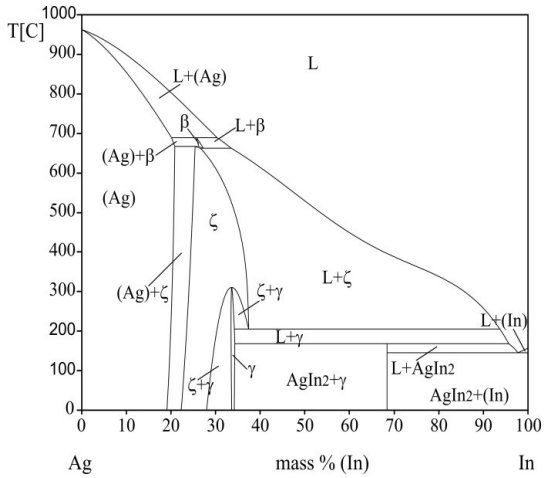

Fig. 1. Calculated phase diagram of the binary Ag-In system [1]

In contrast to an assessment carried out by *Liu et al.* [14] in which used thermodynamic data for the binary Ag-In system were taken from *Moser et al.* [28], in the current study corrected data for binary Ag-In system from COST 531 database [1] were used. This will most probably lead to difference in phase diagrams presented in this study to that of *Liu et al.* [14] and it is to this difference that investigation of ternary Ag-Bi-In system is necessary.

A list of considered phases of the ternary Ag-Bi-In system with their corresponding Pearson symbols is presented in Table 1.

Table 1. Considered phases, their crystallographic data and database names

Thermodynamic database name	Common name	Space group symbol	Strukturbericht designation	Pearson's symbol
LIQUID	Liquid	-	-	-
FCC_A1	(Ag)	$Fm\bar{3}m$	A1	*cF4*
RHOMBO_A7	(Bi)	$R\bar{3}m$	*A*7	*hR*2
TETRAG_A6	(In)	*I*4/*mmm*	*A*6	*tI*2
BIIN	BiIn	*P*4/*nmms*	*B*10	*tP*4
BI3IN5	Bi_3In_5	*I*4/*mcm*	$D8_1$	*tI*32
BIIN_BRASS	$BiIn_2$	$P6_3/mmc$	$B8_2$	*hP*6
TET_ALPHA1	ε	*I*4/*mmm*	*A*6*mod*	*tI*2
BCC_A2	β (Ag_3In)	$Pm\bar{3}m$	*A2*	*cP2*
HCP_A3	ζ (Ag_3In)	$P6_3/mmc$	*A3*	*hP2*
AGIN2	$AgIn_2$	*I*4/*mcm*	*C16*	*tI12*
CUIN_GAMMA	γ (Ag_2In)	$P\bar{4}3m$	$D8_{1\text{-}3}$	*cP52*

Results and discussion

The applied investigation techniques were on one hand selected in a manner to provide adequate experimental data on which theoretical predictions can be based and on the other to provide necessary data for validation of thermodynamic calculations.

DTA analysis was carried out on the five alloy samples from x(Ag)=0.5 vertical section. Experimentally determined phase transition temperatures are given in Table 2 along with the results of thermodynamic calculations i.e. calculated phase transition temperatures.

Table 2. Comparative presentation of the experimentally determined (DTA) and the calculated phase transition temperatures

Alloy composition (mass %)	Phase transition temperatures (°C)			
	Invariant reaction and other peak temperature		Liquidus temperature	
	Experimental	Calculated	Experimental	Calculated
$Ag_{50}Bi_{10}In_{40}$	101.2; 282,6	96.1; 277.8	551.6	553.2
$Ag_{50}Bi_{20}In_{30}$	113.2; 230.2; 269.1	108.4; 231.7; 268.4	572.4	569.8
$Ag_{50}Bi_{24.4}In_{25.6}$	204.8	196.7	568.2	571
$Ag_{50}Bi_{30}In_{20}$	233.6; 517.6	231.7; 521.4	571	578
$Ag_{50}Bi_{40}In_{10}$	259.4	261.4	604.4	598

Comparison between calculated vertical section based on data from COST 531 database [1], experimentally determined phase transition temperatures and literature data is given on Fig. 2.

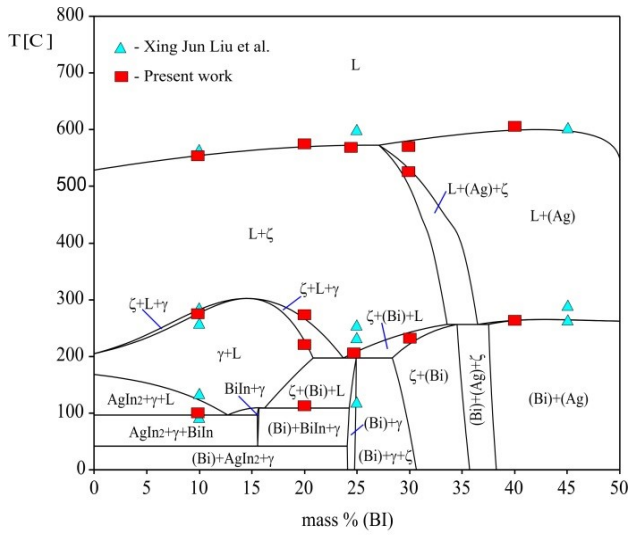

Fig. 2. Predicted vertical section x(Ag)=0.5 of the ternary Ag-Bi-In system compared with DTA results from the present study and literature data [14]

The calculated vertical section (Fig. 2) shows close agreement with the experimentally obtained results (DTA) from this study, both for liquidus and solidus temperatures. Furthermore, an overall agreement between the calculated phase diagram

and the data reported by *Liu et al.* [14] can be observed as well. Although in the Bi rich region there is some discrepancy between calculated and experimentally determined temperatures on one side and data given by *Liu et al.* [14] on the other.

The calculated isothermal section of the Ag-Bi-In ternary system at 100 ºC is presented on Fig. 3. Out of thirteen predicted regions that can be observed in the isothermal section at 100 ºC (Fig. 3), nine were further experimentally investigated. Five regions were studied using SEM-EDS and XRD analyzes and six by light optical microscopy. Apart from the results of the calculations, on Fig. 3 are also marked experimentally determined compositions of the investigated alloy samples. The six alloy samples marked with Hindu-Arabic numerals (samples 1 to 6) were investigated using SEM-EDS and XRD analysis while the samples marked with Roman numerals (I to VI) were studied using optical microscopy.

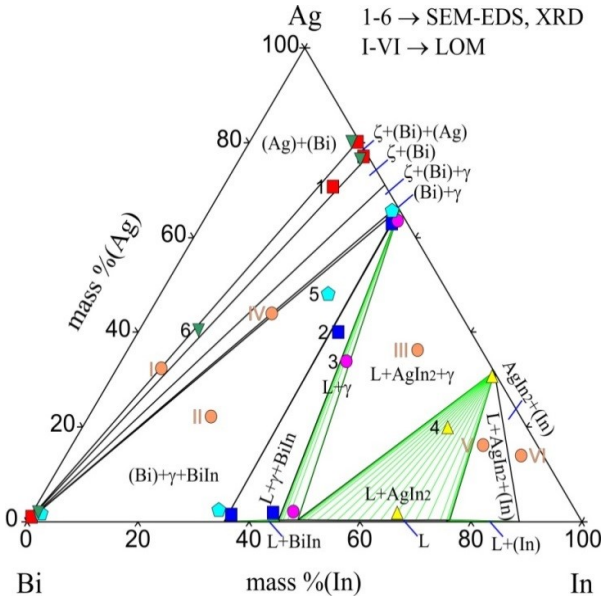

Fig. 3. Predicted phase diagram of the Ag-Bi-In ternary system at 100 °C with experimentally determined (SEM-EDS) overall alloy and individual phase compositions

The experimentally determined phase compositions of the studied alloys and the chemical compositions of the identified phases are given in Table 3 and compared with thermodynamically predicted compositions.

Table 3. SEM-EDS results: experimentally determined phase compositions of the investigated alloys of the ternary Ag-Bi-In system in comparison with thermodynamic predictions

Sample	Overall exp. composition (mass %)	Coexisting phases		Compositions of the phases (mass %)					
		Predicted	SEM-EDS	Ag		In		Bi	
				Exp.	Cal.	Exp.	Cal.	Exp.	Cal.
1.	70 Ag 20 In 10 Bi	(Bi) ζ (Ag)	(Bi) ζ (Ag)	1.47±0.3 77.96±0.3 80.21±0.1	- 77.09 80.47	0.29±0.4 21.34±0.2 19.37±0.6	- 22.9 19.53	98.24±0.7 0.7±0.4 0.42±0.1	100 0.01 -
2.	40 Ag 36 In 24 Bi	Liquid BiIn γ	Liquid BiIn γ	1.79±0.2 0.33±0.6 64.42±0.4	0.3 - 65.81	43.51±0.6 36.1±0.3 34.25±0.4	45.11 35.46 34.19	54.7±0.4 63.57±0.1 1.33±0.1	54.59 64.54 -
3.	34 Ag 41 In 25 Bi	Liquid γ	Liquid γ	1.94±0.3 63.25±0.3	0.32 65.8	46.54±0.5 35.55±0.7	45.54 34.2	51.52±0.2 1.2±0.1	53.14 -
4.	20 Ag 66 In 14 Bi	$AgIn_2$ Liquid	$AgIn_2$ Liquid	29.56±0.5 0.62±0.4	31.63 0.28	69.17±0.2 65.9±0.4	68.37 65.04	1.27±0.3 33.48±0.3	- 34.68
5.	48 Ag 30 In 22 Bi	BiIn (Bi) γ	BiIn (Bi) γ	2.09±0.1 0.48±0.4 65.97±0.1	- - 65.97	33.89±0.5 0.78±0.1 32.77±0.8	35.46 - 34.03	64.02±0.5 98.74±0.4 1.32±0.1	64.54 100 -
6.	40 Ag 11 In 49 Bi	(Bi) ζ (Ag)	(Bi) ζ (Ag)	1.35±0.2 76.84±0.3 80.23±0.2	- 77.09 80.47	0.84±0.2 22.04±0.3 18.78±0.7	- 22.9 19.53	97.81±0.4 1.11±0.1 0.98±0.2	100 0.01 -

From the results given in Table 3 it can be seen that the presence of all of the predicted phases was experimentally confirmed. SEM images of microstructures of the six studied alloy samples are presented on Fig. 4. The present phases identified using results of energy dispersive spectrometry (EDS) analysis are marked on the presented microstructures.

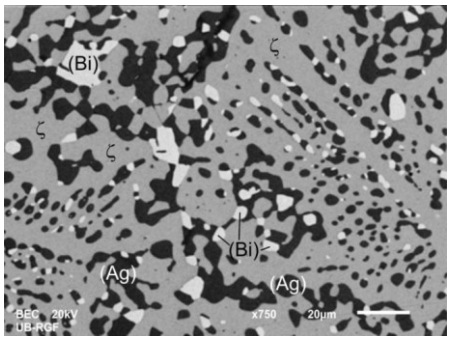

1)

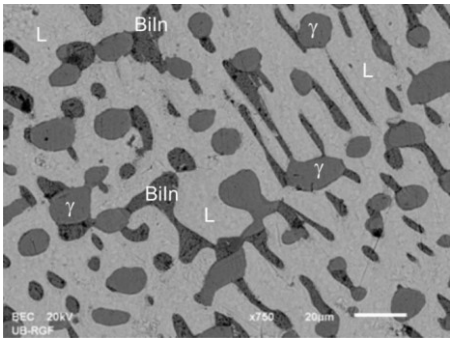

2)

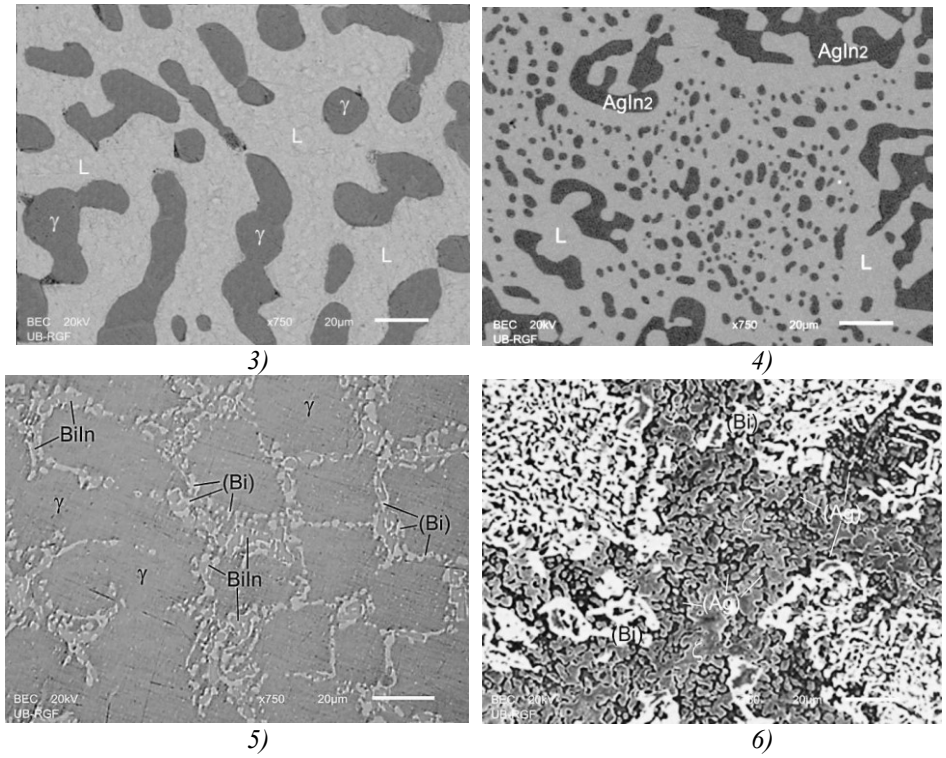

Fig. 4. SEM micrographs of the alloy samples: 1) $Ag_{70}Bi_{10}In_{20}$, 2) $Ag_{40}Bi_{24}In_{36}$, 3) $Ag_{34}Bi_{25}In_{41}$, 4) $Ag_{20}Bi_{14}In_{66}$, 5) $Ag_{48}Bi_{22}In_{30}$, and 6) $Ag_{40}Bi_{49}In_{11}$ (mass %)

The alloy samples 1 and 6 belong to a same (Bi)+ζ+(Ag) three-phase region, and in the both presented microstructures the solid solution (Bi) appears as light colored grains, the intermetallic compound ζ as gray phase and the solid solution (Ag) as a dark phase trapped between (Bi) and ζ grains. The sample 2 belongs to a Liquid+BiIn+γ three-phase region and the all three predicted phases were detected within the studied microstructure. The samples 3 and 4 are from two different two-phase regions. Within the microstructures of the both samples liquid phase appears as a light-gray phase while the second phase appears as dark-gray grains with well-defined boundaries. The sample 5 is from BiIn+(Bi)+γ three phase region and as expected, the presented microstructure (Fig. 4) reveals a solid solution (Bi) phase in which lay BiIn and γ phases.

Phase composition of the studied alloy samples was further analyzed using XRD technique and the obtained results are shown in Table 4.

Table 4. Results of XRD analysis: identified phases and calculated corresponding lattice parameters compared with literature data [23, 29-33]

S.	Overall exp. Composition (mass %)	Coexisting phases		Lattice parameters (Å)			
		SEM-EDS	XRD	*a=b*		*c*	
				Exp.	Ref.	Exp.	Ref.
1.	70 Ag 20 In 10 Bi	(Bi) ζ (Ag)	(Bi) ζ (Ag)	4.5479(2) 2.9556(2) 4.1487(3)	4.548 [29] 2.9563 [30] 4.1497 [31]	11.8534(3) 4.7863(2)	11.852 [29] 4.7857 [30]
2.	40 Ag 36 In 24 Bi	Liquid BiIn γ	- BiIn γ	- 4.9732(4) 9.9276(3)	 4.972 [32] 9.922 [33]	4.8299(5)	4.83 [32]
3.	34 Ag 41 In 25 Bi	Liquid γ	- γ	- 9.9244(3)	 9.922 [33]		
4.	20 Ag 66 In 14 Bi	Liquid $AgIn_2$	- $AgIn_2$	- 6.8703(2)	 6.869 [23]	5.6038(6)	5.604 [23]
5.	48 Ag 30 In 22 Bi	BiIn (Bi) γ	BiIn (Bi) γ	4.9731(1) 4.5487(3) 9.9228(4)	4.972 [32] 4.548 [29] 9.922 [33]	4.8277(6) 11.8526(1)	4.83 [32] 11.852 [29]
6.	40 Ag 11 In 49 Bi	(Bi) ζ (Ag)	(Bi) ζ (Ag)	4.5474(5) 2.9569(1) 4.1503(3)	4.548 [29] 2.9563 [30] 4.1497 [31]	11.8596(2) 4.7863(1)	11.852 [29] 4.7857 [30]

As can be seen from Table 4, the obtained results confirm presence of the phases determined by SEM-EDS analysis. It can also be said that the determined values of lattice parameters for (Bi), ζ, (Ag), BiIn, γ, $AgIn_2$ phases are in close agreement with literature data [23, 29-33].

As previously stated, the six alloy samples marked with Roman numerals on Fig. 3 were studied using optical microscopy. From Fig. 3, it can be seen that all of the six samples belong to different regions i.e. the samples I, II, III and V are from three-phase regions while the samples IV and VI are from two-phase regions. Microstructures of the studied alloy samples are illustrated by metallographic images presented on Fig. 5. In line with the thermodynamic predictions in the microstructures of the samples I, II, III and V (Fig. 5) three phases can be observed and only two phases in the microstructures of the samples IV and VI. According to the results of thermodynamic calculations it can be assumed that the observed phases in the microstructure of the alloy sample I are most probably (Bi), ζ and (Ag), in the sample II ((Bi), γ and BiIn phase), in the sample III (L, AgIn2 and γ), also in the sample IV ((Bi) and γ), in the sample V (L, $AgIn_2$ and (In)) and in the sample VI ($AgIn_2$ and (In)).

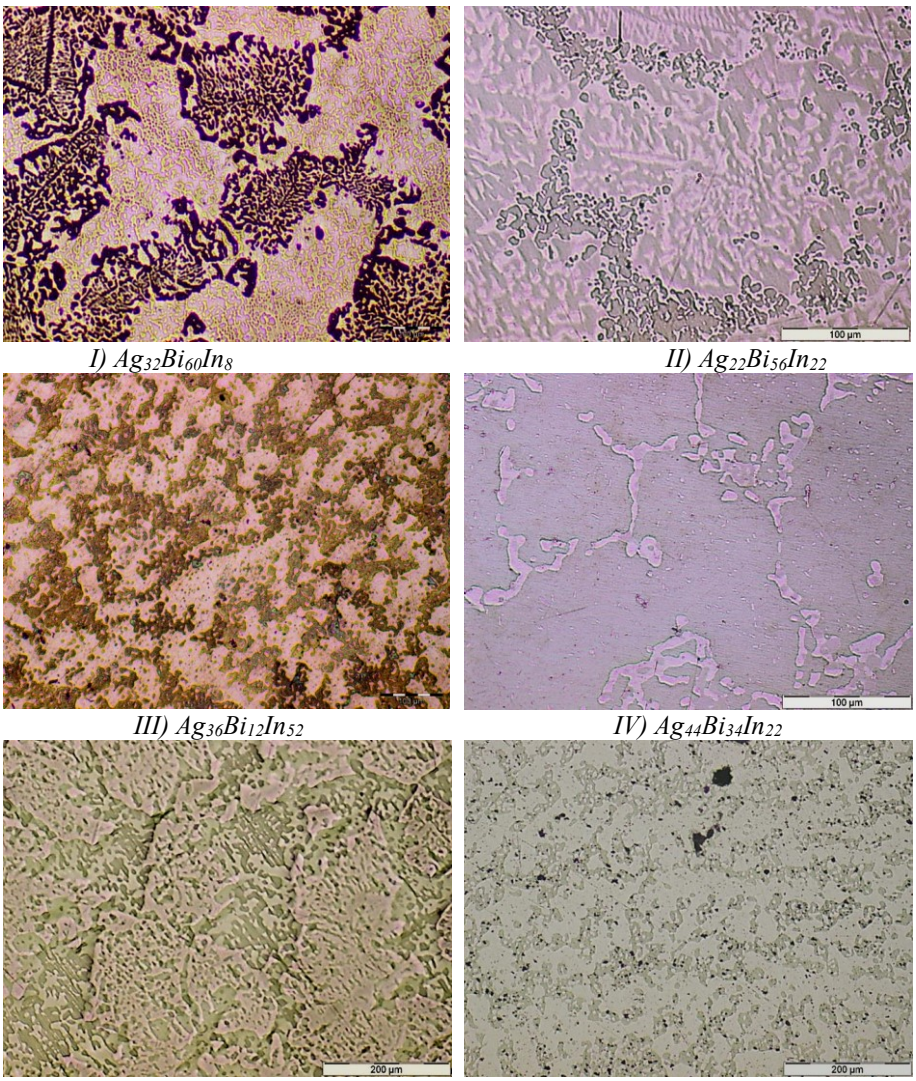

I) $Ag_{32}Bi_{60}In_8$ *II) $Ag_{22}Bi_{56}In_{22}$*

III) $Ag_{36}Bi_{12}In_{52}$ *IV) $Ag_{44}Bi_{34}In_{22}$*

V) $Ag_{16}Bi_{10}In_{74}$ *VI) $Ag_{14}Bi_4In_{82}$*

Fig. 5. Microstructures of the selected alloy samples from the ternary Ag-Bi-In system: I) $Ag_{32}Bi_{60}In_8$, II) $Ag_{22}Bi_{56}In_{22}$, III) $Ag_{36}Bi_{12}In_{52}$, IV) $Ag_{44}Bi_{34}In_{22}$, V) $Ag_{16}Bi_{10}In_{74}$ and VI) $Ag_{14}Bi_4In_{82}$ (mass %)

A liquidus surface projection of the ternary Al-Bi-In system predicted by thermodynamic calculations is presented in Fig. 6. Two large regions ((Ag) and ζ) and nine smaller primary crystallization fields ((Bi), (In), BiIn, Bi_3In_5, $BiIn_2$, γ, ε, β and $AgIn_2$) can be observed on the predicted liquidus projection. With the purpose of making smaller regions more visible enlarged part of the liquidus surface in the vicinity of binary Bi-In system is given as an insert in Fig. 6.

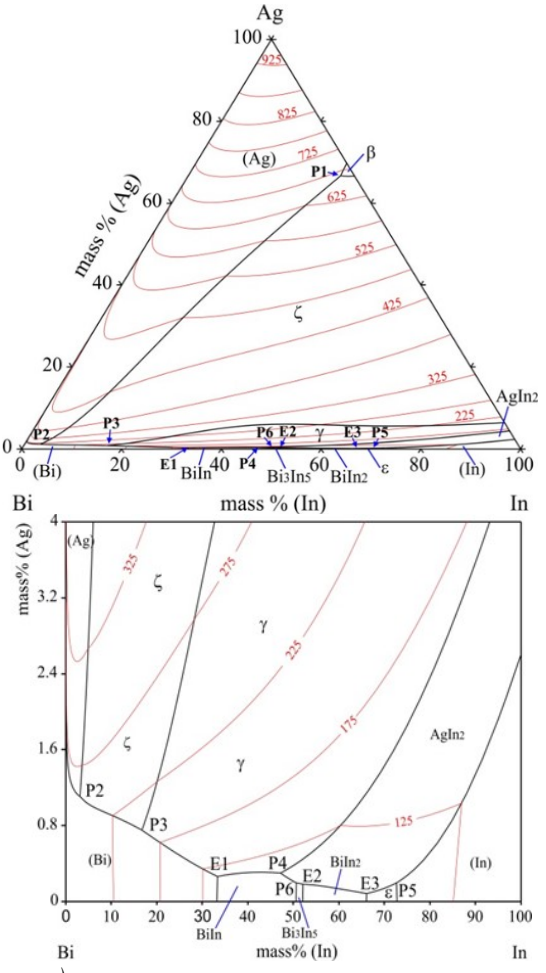

a) *b)*

Fig. 6. Calculated liquidus projection of the ternary Ag-Bi-In system: a) surface of liquidus projection, b) magnified part of the liquidus surface in the vicinity of Bi-In binary system

In comparison to previously defined liquidus projection given by *Liu et al.* [14], some differences can be observed, for instance larger solubility of Ag in γ phase and existence of a new phase β. The calculations predict invariant reactions to take place at slightly lower temperatures than that reported by *Liu et al.* [14] and also predict existence of a one high temperature invariant reaction P1 (see Table 5) which represents formation of β phase.

According to the obtained results of thermodynamic calculations there are altogether nine invariant reactions in the Ag-Bi-In ternary system. The predicted invariant reactions are listed in Table 5, three of them are E-type reactions and the other six are P-type reactions.

Table 5. Predicted invariant reactions in the ternary Ag-Bi-In system

	T(°C)	Reaction	Phase	Composition (at. %)			Type
				Ag	Bi	In	
1.	665.59	L + ζ ↔ (Ag) + β	L ζ (Ag) β	68.83 75.75 80.15 74.89	1.51 0.09 0.07 0.14	29.66 24.16 19.78 24.97	P1
2.	255.98	L + (Ag) ↔(Bi) + ζ	L (Ag) (Bi) ζ	2.07 80.85 - 77.23	92.55 0.16 99.99 0.26	5.38 18.99 0.01 22.51	P2
3.	196.78	L + ζ ↔ (Bi)+ γ	L ζ (Bi) γ	1.27 70.99 - 67.95	72.21 0.09 99.99 -	26.52 28.92 0.01 32.05	P3
4.	108.47	L ↔ (Bi) + γ+ BiIn	L (Bi) γ BiIn	0.39 - 67.38 -	52.12 99.99 - 50	47.49 0.01 32.62 50	E1
5.	96.10	L + γ ↔ BiIn + $AgIn_2$	L γ BiIn $AgIn_2$	0.42 67.17 - 33	37.85 - 50 -	61.73 32.83 50 67	P4
6.	89.54	L + (In) ↔$AgIn_2$ + ε	L (In) $AgIn_2$ ε	0.24 - 33 -	17.03 7.95 - 10.05	82.73 92.05 67 89.95	P5
7.	88.13	L + BiIn ↔ $AgIn_2$ + Bi_3In_5	L BiIn $AgIn_2$ Bi_3In_5	0.26 - 33 -	34.75 50 - 37.5	64.99 50 67 62.5	P6
8.	87.21	L ↔ $AgIn_2$ + Bi_3In_5 + $BiIn_2$	L $AgIn_2$ Bi_3In_5 $BiIn_2$	0.24 33 - -	33.45 - 37.5 33.33	66.31 67 62.5 66.67	E2
9.	71.46	L ↔ $AgIn_2$ + $BiIn_2$+ ε	L $AgIn_2$ $BiIn_2$ ε	0.1 33 - -	21.98 - 33.33 15.26	77.92 67 66.67 84.74	E3

Information about the hardness of the alloys of the ternary Ag-Bi-In system was obtained using Brinell test method. Studied alloy samples were selected from three vertical sections Bi-$Ag_{0.25}In_{0.75}$, Bi-AgIn and Bi-$Ag_{0.75}In_{0.25}$. The obtained values of the Brinell hardness of the studied alloy samples are given in Table 6, along with experimentally obtained values for three binary alloys and literature values of hardness of the pure elements [34].

Based on the experimentally obtained values of Brinell hardness listed in Table 6 and an appropriate mathematical model iso-lines of hardness were predicted for all ternary alloys of the Ag-Bi-In system at 100 °C.

Table 6. Brinell hardness of the studied alloy samples from the ternary Ag-Bi-In system

Brinell hardness HB (MN/m^2)						
Mole fraction of components			Measured values			Mean value
x(Ag)	x(Bi)	x(In)	1	2	3	
Bi-$Ag_{0.25}In_{0.75}$						
0.25	0	0.75	65.4	65.5	65.3	65.4
0.2	0.2	0.6	42.2	42.8	41.6	42.2
0.15	0.4	0.45	23.1	23.2	23.3	23.2
0.1	0.6	0.3	33.0	29.8	26.7	29.8
0.005	0.8	0.15	31.8	35.7	36.0	34.5
Bi-AgIn						
0.5	0	0.5	62.9	62.5	63	62.8
0.4	0.2	0.4	27.1	28.4	30.5	28.6
0.3	0.4	0.3	38.3	42.1	44.7	41.7
0.2	0.6	0.2	18.6	18.4	18.2	18.4
0.1	0.8	0.1	25.4	22.4	21.8	23.2
Bi-$Ag_{0.75}In_{0.25}$						
0.75	0	0.25	39.5	38.2	38.4	38.6
0.6	0.2	0.2	19.1	20.1	19.1	19.4
0.45	0.4	0.15	23.8	21.4	22.8	22.6
0.3	0.6	0.1	24.8	24.1	23.7	24.2
0.15	0.8	0.005	26.7	25.4	27.1	26.4
0	1	0	94.2			94.2 [34]
1	0	0	24.5			24.5 [34]
0	0	1	8.83			8.83 [34]

The applied mathematical model was defined using Design Expert v.9.0.3.1 software package. Out of possible canonical or Scheffe models [35-37] that meet the requirements of adequacy a cubic mixture model is recommended:

$$\hat{y} = \sum_{i=1}^{q} \beta_i x_i + \sum_{i<j}^{q-1} \sum_{j}^{q} \beta_{ij} x_i x_j + \sum_{i<j}^{q-1} \sum_{j}^{q} \delta_{ij} x_i x_j (x_i - x_j) + \sum_{i<j}^{q-2} \sum_{j<k}^{q-1} \sum_{k}^{q} \beta_{ijk} x_i x_j x_k \quad (1)$$

The Analysis of variance (ANOVA) confirms the adequacy of the model. The determined F-value of the model is 15.086, which implies that the model is significant. There is only a 0.01% chance that the ”Model F-Value“ this large could occur due to noise. Hence, the final equation of the predictive model in terms of actual components is:

$$HB(MN/m^2)==24.99217 \cdot x(Ag)+74.23516 \cdot x(Bi)+9.322171 \cdot x(In)-152.46 \cdot x(Ag) \cdot x(Bi) +172.782 \cdot x(Ag) \cdot x(In)-104.323 \cdot x(Bi) \cdot x(In)+92.70894 \cdot x(Ag) \cdot x(Bi) \cdot x(In)+ 105.426 \cdot x(Ag) \cdot x(Bi) \cdot (x(Ag)-x(Bi))-196.725 \cdot x(Ag) \cdot x(In) \cdot (x(Ag)-x(In))- 73.8202 \cdot x(Bi) \cdot x(In) \cdot (x(Bi)-x(In)) \quad (2)$$

Iso-lines contour plot of the Brinell hardness of the alloys from the Ag-Bi-In system at 100 °C defined by equation 2 is presented on Fig. 7.

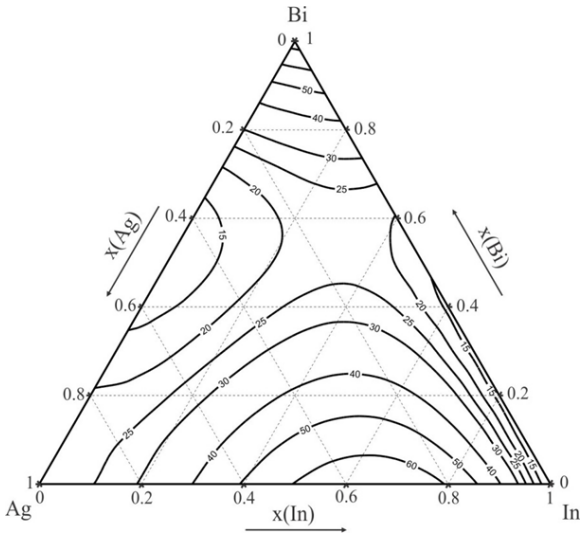

Fig. 7. Iso-lines of Brinell Hardness for alloys of the ternary Ag-Bi-In system at 100 °C

The same alloy samples were used for electrical conductivity measurements and the experimentally determined values together with values of electrical conductivity of the pure elements [38] are listed in Table 7.

Table 7. Electrical conductivities of the selected alloys from the isothermal section at 100 °C

Electrical conductivity (MS/m)							
Mole fraction of components			Measured values				Mean value
x(Ag)	x(Bi)	x(In)	1	2	3	4	
$Bi\text{-}Ag_{0.25}In_{0.75}$							
0.25	0	0.75	14.71	14.70	14.75	14.85	14.75
0.2	0.2	0.6	1.853	1.850	1.839	1.804	1.837
0.15	0.4	0.45	0.769	0.791	0.768	0.735	0.766
0.1	0.6	0.3	0.988	0.981	0.981	0.981	0.983
0.05	0.8	0.15	0.332	0.301	0.307	0.296	0.309
Bi-AgIn							
0.5	0	0.5	12.13	12.06	11.94	12.12	12.06
0.4	0.2	0.4	1.919	1.975	2.011	2.201	2.027
0.3	0.4	0.3	1.323	1.328	1.339	1.354	1.336
0.2	0.6	0.2	1.941	1.963	1.925	1.933	1.941
0.1	0.8	0.1	0.441	0.442	0.441	0.443	0.442
$Bi\text{-}Ag_{0.75}In_{0.25}$							
0.75	0	0.25	19.24	18.26	18.25	18.24	18.50
0.6	0.2	0.2	4.827	4.835	4.961	4.823	4.862
0.45	0.4	0.15	1.274	1.291	1.286	1.311	1.291
0.3	0.6	0.1	1.019	1.074	0.9773	1.039	1.027
0.15	0.8	0.05	0.4595	0.455	0.4402	0.446	0.4502
0	1	0	0.769				0.769 [38]
1	0	0	62				62 [38]
0	0	1	11.6				11.6 [38]

Calculations of electrical conductivity of the alloys from the Ag-Bi-In ternary system at 100 °C were carried out in the same manner as the previously mentioned Brinell hardness calculations. The final equation of the predictive model in terms of actual components is:

$$\sigma(\text{MS/m})=61.25589\cdot x(\text{Ag})-2.5012\cdot x(\text{Bi})+10.85589\cdot x(\text{In})-114.163\cdot x(\text{Ag})\cdot x(\text{Bi})-101.392\cdot x(\text{Ag})\cdot x(\text{In})-39.1753\cdot x(\text{Bi})\cdot x(\text{In})+164.4702\cdot x(\text{Ag})\cdot x(\text{Bi})\cdot x(\text{In})-82.2624\cdot x(\text{Ag})\cdot x(\text{Bi})\cdot(x(\text{Ag})\cdot x(\text{Bi}))-113.394\cdot x(\text{Ag})\cdot x(\text{In})\cdot(x(\text{Ag})\cdot x(\text{In}))+64.05992\cdot x(\text{Bi})\cdot x(\text{In})\cdot(x(\text{Bi})\cdot x(\text{In})) \quad (3)$$

The resulting iso-lines contour plot of the electrical conductivity defined by equation 3 is shown on Fig. 8.

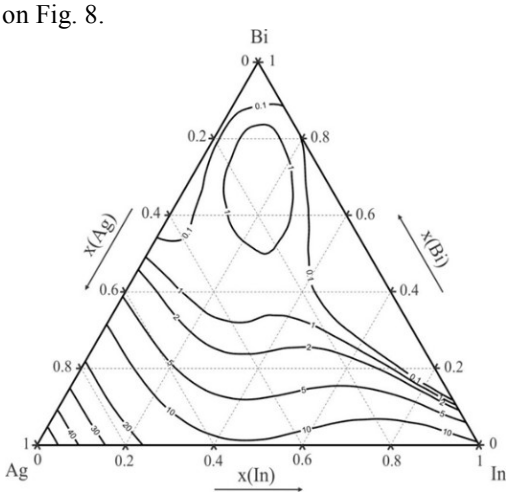

Fig. 8. Iso-lines of electrical conductivity of the ternary Ag-Bi-In system at 100 °C

The ternary alloy samples from isothermal section at 100 °C were further studied in terms of hardness of the individual phases. The values of measured Vickers microhardness are marked on micrographs presented on Fig. 9.

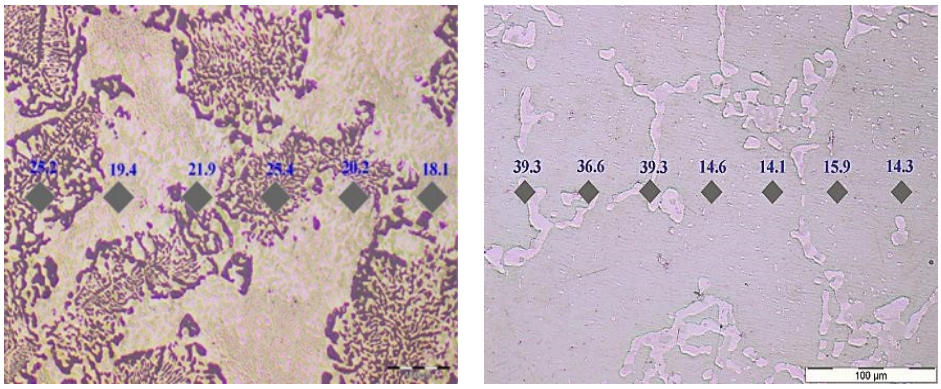

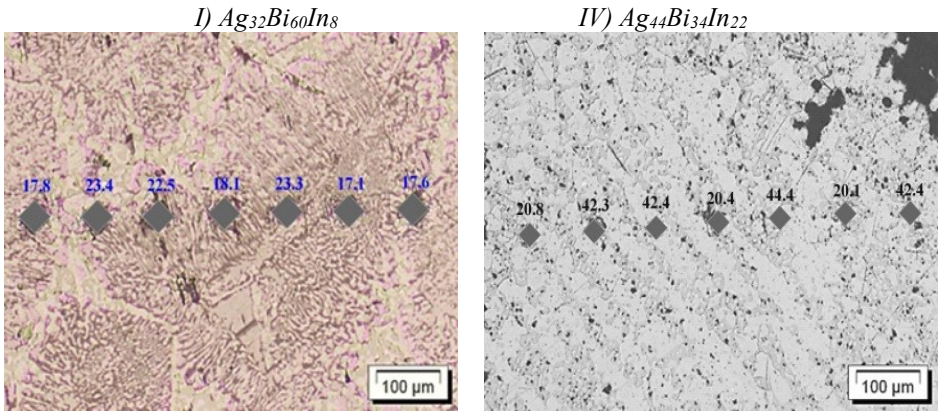

Fig. 9. Micrographs with marked hardness of phases determined by Vickers test: I) $Ag_{32}Bi_{60}In_8$, IV) $Ag_{44}Bi_{34}In_{22}$, V) $Ag_{16}Bi_{10}In_{74}$ and VI) $Ag_{14}Bi_4In_{82}$ (mass %)

Micro Vickers tests were carried out on the same four alloy samples that were studied by light optical microscopy. As previously determined, the two samples are from three-phase regions and two are from two-phase regions. Although, in the microstructure of the sample I three phases were found (ζ, (Bi) and (Ag)), the solid solutions (Ag) and (Bi) are mixed together and the hardness measurement for the each individual phase was not possible. Nevertheless, it was found that the hardness of the mixture of these two solid solutions is in range 18.1 to 21.9 MN/m^2. The lower hardness values can be ascribed to presence of larger amounts of the solid solution (Ag). The third identified phase (ζ) appears as small grains dispersed in a matrix of the solid solutions (Ag) and (Bi). The measured value of hardness of this phase is in range 25.2 to 25.4 MN/m^2.

The sample IV belongs to the (Bi)+γ two phase region. Considering that its microstructure is clearly divided into separate grains i.e. grain boundaries are well defined the hardness measurements for individual phases were carried out. Measured hardness of the solid solution (Bi) is in range 14.1 to 15.9 MN/m^2 whereas hardness of the γ phase is 39.3 MN/m^2. In the microstructures of the samples V and VI presence of a solid solution (In) and an intermetallic compound $AgIn_2$ was detected. In addition to these two phases in the microstructure of the sample V a liquid phase was detected as well. Given that the all three phases have rather small grains hardness measurements for the individual phases were not possible. An overall hardness for this sample was found to be in a range between 17.1 and 23.4 MN/m^2. In case of the sample VI, measured values of hardness for the solid solution (In) were from 20.1 to 20.8 MN/m^2 and for the $AgIn_2$ intermetallic compound from 42.4 to 44.4 MN/m^2.

Conclusions

Alloys from the ternary Ag-Bi-In system at 100 °C were studied in terms of mechanical and electrical properties. In addition, isothermal section at 100 °C liquidus surface, invariant reactions and vertical section x(Ag)=0.5 were thermodynamically assessed and experimentally investigated.

The experimentally obtained results of EDS and XRD analyses support the results of thermodynamic calculations as they were found to be in a close agreement with the predicted phase diagram at 100 °C. The lattice parameters of the identified phases determined using XRD analysis were found to match literature data quite well.

A close agreement was also obtained between the calculated vertical section x(Ag)=0.5 and experimentally obtained results (DTA), both for liquidus and solidus temperatures. Also, a good overall agreement with known literature data was obtained.

Thermodynamic calculations of the liquidus surface based on new data from COST 531 database have revealed existence of eleven regions of primary crystallization and nine invariant reactions. As expected, despite overall agreement with known literature data on liquidus projection some differences were observed e.g. larger solubility of Ag in γ phase and existence of a new phase β. Furthermore, the calculations predict invariant reactions to take place at slightly lower temperatures than stated in literature and also predict existence of the additional high temperature invariant P-type reaction, which corresponds to formation of β phase.

Conducted Vickers micro hardness measurements have provided some additional information on hardness of the phases present in the microstructure of the four selected alloy samples. The highest value was measured for $AgIn_2$ intermetallic compound which was found to be in a range between 42.4 and 44.4 MN/m^2.

Brinell hardness and electrical conductivity were experimentally determined for the selected alloys from the three studied vertical sections (Bi-$Ag_{0.25}In_{0.75}$, Bi-AgIn and Bi-$Ag_{0.75}In_{0.25}$) of the ternary Ag-Bi-In system. Using appropriate mathematical model and experimentally obtained results, values of Brinell hardness and electrical conductivity for all ternary alloys of the Ag-Bi-In system at 100 °C were predicted.

Acknowledgement

This work was supported by the Ministry of Education, Science and Technological Development of the Republic of Serbia, under Project No. ON172037.

References

[1] A. Kroupa, A.T. Dinsdale, A. Watson, J. Vřeštál, J. Vızdal, A. Zemanová: JOM-US, 59 (2007) 20-25.

[2] A. Dinsdale, A. Kroupa, A. Watson, J. Vřeštál, A. Zemanová, P. Brož, Handbook of high-temperature lead-free solders, vol. 1: Atlas of phase diagrams, COST office (2012).

[3] D. Soares, C. Vilarinho, J. Barbosa, F. Samuel, L. Trigo, P. Bre: J. Min. Metall Sect B-Metall, 43 (2007) 131-139.

[4] J. Sopoušek, J. Vřeštál, A. Zemanová, J. Buršik: J Min Metall Sect B-Metall, 48 (2012) 419-425.

[5] A.T. Wu, K.H. Sun: J. Electron. Mater., 38(12) (2009) 2780-2785.

[6] A. Sabbar, A. Zrineh, J. P. Dubes, M. Gambino, J. P. Bros, G. Borzone: Thermochim Acta, 395 (2003) 47-58.

[7] V. Vassiliev, M. Alaoui-Elbelghiti, A. Zrineh, M. Gambino, J.P. Bros: J Alloy Compd, 265 (1998) 160-169.

[8] Z. Li, Z. Cao, S. Knott, A. Mikula, Y. Du, Z. Qiao: Calphad, 32 (2008) 152-163.

[9] U.R. Kattner, W.J. Boettinger: J Electron Mater, 23 (1994) 603-610.

[10] W. Chen, L. Zhang, Y. Du: Calphad, 52 (2016) 159-168.
[11] A. Milosavljević, D. Živković, Ž. Kamberović: Metalurgija-J Metall, 14 (2008) 161-167.
[12] N. Moelans, K. C. Hari Kumar, P. Wollants: J Alloy Compd, 360 (2003) 98-106.
[13] V.T. Witusiewicz, U. Hecht, B. Böttger, S. Rex: J Alloy Compd, 428 (2007) 115-124.
[14] X.J. Liu, T. Yamaki, I. Ohnuma, R. Kainuma, K. Ishida: Mater Trans, 45 (2004) 637-645.
[15] K. Kameda, K. Yamaguchi: J Jpn Inst Met, 55 (1991) 536-544.
[16] H.J. Snyder: T Metall Soc Aime, 239 (1967) 1385-1391.
[17] T. Satow, O. Uemura, S. Yamakwa: Trans Jpn Inst Met, 15 (1974) 253-255.
[18] H. Ohtani, I. Satou, M. Miyashita, K. Ishida: Mater Trans, 42 (2001) 722-731.
[19] E. Zoro, C. Servant, B. Legendre: Calphad, 31 (2007) 89-94.
[20] Y. Cui, S. Ishihara, X.J. Liu, I. Ohnuma, R. Kainuma, H. Ohtani, K. Ishida: Mater Trans, 43 (2002) 1879-1886.
[21] D. Boa, I. Ansara: Thermochim. Acta, 314 (1998) 79-86.
[22] F. Weibke: A Anorg Chem, 222 (1935) 145-160.
[23] E. Hellner: Z. Metallkd, 42 (1951) 17-19.
[24] L.L. Frevel, E. Ott: J Am Chem Soc, 57 (1935) 228-233.
[25] A.N. Campbell, R. Wagemann, R.B. Ferguson: Can J Chem, 48 (1970) 1703-1715.
[26] M.R. Baren, Indium Alloys and their engineering applications, ed. C.E.T. White and H. Okamoto materials Park, OH, ASM Intl. (1993).
[27] T.M. Kornenhen, J.K. Kivilahti: J Electron Mater, 27 (1998) 149-155.
[28] Z. Moser, W. Gasior, J. Pstrus, W. Zakulski, I. Ohnuma, X.J. Liu, Y. Inohana, K. Ishida: J Electron Mater, 30 (2001) 1120-1128.
[29] W.P. Davey: Phil Mag 6 (47) (1924) 657-671.
[30] H.W. King, T.B. Massalski: Phil Mag, 6 (1961) 669-682.
[31] M.E. Straumanis, S.M. Riad: T Metall Soc Aime, 233 (1965) 964-967.
[32] R. Kubiak: Z Anorg Allg Chem, 431 (1977) 261-267.
[33] J.K. Brandon, R. Brezard, W.B. Pearson, D.J.N. Tozer: Acta Crystallogr, B 33 (1977) 527-537.
[34] http://www.webelements.com/periodicity/hardness_brinell/, Accessed 20 February 2017.
[35] J.A. Cornell: Experiments with Mixtures, 3rd Ed., John Wiley&Sons, Inc, New York (2002)
[36] Ž. Lazić, Design of Experiments in Chemical Engineering, Wilez-VCH Verlag GmbH&Co.KGaA, Weiheim (2004).
[37] M. Kolarević, M. Vukićević, B. Radičević, M. Bjelić, V. Grković, In: Proceedings of the Seventh Triennial International Conference Heavy Machinery (2011) 1-6.
[38] http://periodictable.com/Properties/A/ElectricalConductivity.an.html, Accessed 20 February 2017.